The Effect of Cirrus Clouds on 8–13-μ Infrared Sky Radiance

Freeman F. Hall, Jr.

An experimental investigation of ir sky radiance and radiance fluctuations in the 8–13-μ atmospheric window is reported. Measurements were made with ground-based, filtered bolometer detector radiometers under clear sky and cirrus overcast conditions. Sky radiance was measured very close to the limb of the sun to permit detection of the solar aureole caused by forward scattering by cirrus ice crystals. Polarized sky radiance was found at large zenith angles and is attributed to scattering by cirrus of thermal emission from the earth. The radiance due to tropospheric water vapor is predicted by means of a radiation chart. Measurements of clear sky radiance exceeded that predicted by the chart in all but one case. The radiance of visible cirrus greatly exceeds the radiation chart prediction. Diffraction about cirrus cloud particles leads to a prediction of a solar aureole of a size that corresponds to the measured aureole. It is concluded that even a cirrus haze, which is quite difficult for an unaided, ground-based observer to detect, can cause an excess zenith radiance of 0.1 mW $cm^{-2}sr^{-1}$, which increases to twice this value at a zenith angle of 60°. Even thin but visible cirrus clouds can easily produce an excess zenith radiance of 1 mW $cm^{-2}sr^{-1}$, which increases by a factor 1.4 at a zenith angle of 60°.

Introduction

The objective of this investigation was to determine experimentally the cause of excess fluctuating clear sky ir radiance in the 8–13-μ region. It is concluded that cirrus clouds are the cause.

Strong,[1] Robinson,[2] Westphal,[3] and Bolle[4] have reported that zenith radiance is often greater than would be expected from radiation charts. Radiance fluctuations may also occur which are not associated with known meteorological variables, and radiance may increase with zenith angle out of proportion to radiation chart predictions.

After preliminary measurements with a spectrally filtered ir radiometer were conducted which showed the anomalies could not be due to 9.6-μ ozone band radiance fluctuations, it was hypothesized that thermal emission and scattering of thermal radiation from the earth by thin cirrus clouds might account for the observed effects. Robinson,[5] and Farmer and Key[6] suggested that particulate matter might contribute to ir sky radiance, but they performed no tests to confirm their assumptions.

If scattering in thin cirrus clouds does add to the sky radiance, there should exist means to discriminate the scattered radiance from thermal emission of gaseous or particulate matter in the atmosphere. In the visual region, scattering causes the solar aureole and leads to polarization of the sky light. The question was whether similar effects existed in the ir.

There are significant differences between the electromagnetic environments in the visual and 8–13-μ ir regions. The radiant power received from the sun and the thermal radiant power emitted by the earth may usually be considered as two spectrally independent streams of flux. To illustrate the minor over-all influence of direct solar radiation at 8–13-μ, the sun contributes an irradiance of 2.2×10^{-4} W cm^{-2}, compared with a visual region solar irradiance of 5.3×10^{-2} W cm^{-2}. Thermal emission from the earth provides an 8–13-μ irradiance of 1.3×10^{-2} W cm^{-2} close to the earth, or sixty times that from the sun. In all examples given above, no atmospheric attenuation is assumed.

One might at first conclude that the solar aureole in the ir would be undetectable because of the relatively low solar irradiance, and that thermal emission from the atmosphere would swamp any trace of it. However, since the average cirrus ice crystal has linear dimensions $2a$ of 100 μ or greater, according to Weickmann,[7] the size parameter is $x = 2\pi a/\lambda = 26$ at 12 μ. This large size parameter can lead to a scattering diagram with forward scattering at small angles many orders of magnitude greater than back scattering. One might therefore hope to detect a thin cirrus-produced aureole by performing sky radiance measurements very close to the solar limb.

It was reasoned that sky polarization in the ir should have a significantly different character than at shorter wavelengths. In the visual region, polarization is generally symmetric about a vertical plane through

The author is with the Douglas Advanced Research Laboratories, McDonnell Douglas Corporation, Huntington Beach, California 92646.

Received 20 December 1967.

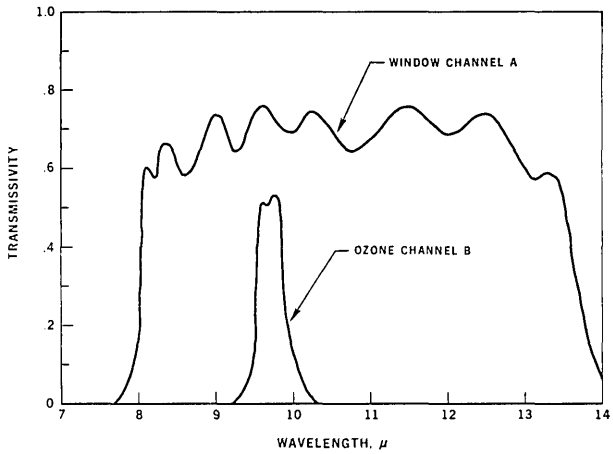

Fig. 1. Transmissivity of the radiometer spectral filters. Channel *A* was filtered to record radiance in the 8.0–13.5-μ window, while Channel *B* monitored 9.6-μ band ozone radiance.

the sun, and the presence of polarization is easy to explain qualitatively because of the nearly parallel rays from the sun and the $(1 + \cos^2 \theta)$ factor to the Rayleigh phase function. In the ir, the source of radiation is the diffuse thermal emission from the solid earth surface, and it is not immediately obvious why this diffuse radiation, coming from a solid angle of 2π sr, should produce polarization in the scattered radiance. This problem is, however, like that of scattering in stellar atmospheres; and Chandrasekhar[8] has shown that for Thomson scattering in an electron stellar atmosphere, polarization is to be expected, increasing toward the limb of the star. Such polarization has been observed in the sun's photosphere,[9] and also in continuum scattering in the chromosphere.[10] Positive polarization might therefore be expected if scattered radiation from cirrus clouds were significant enough to be easily measured. For a uniform cirrus overcast, polarization should be symmetric about any vertical plane, and therefore about the zenith also. It should be independent of the position of the sun.

Radiometric measurements were performed during January and February of 1966 which showed that the 8–13-μ aureole did exist on days when cirrus were present, as well as on a number of apparently clea days, and that ir sky polarization was also detectable. These initial results indicated that a more complete model of infrared sky radiance should include the effects of cirrus clouds, even those thin clouds which the ground-based observer could not easily detect.

Instrumentation

The instrument used to record window sky radiance was a Barnes Engineering Company model R–4B2 dual channel radiometer with bolometer detectors. The data were recorded on a two-channel Sanborn paper tape recorder, which also provided timing marks.

The radiometer is equipped with 1-mm × 1-mm detectors providing a field of view of 25×10^{-6} sr with the standard 10-cm diam $f/2$ optics. The noise equivalent radiance (NEN) is 0.02 mW cm^{-2} sr^{-1} with an electronic bandwidth of 0.1 Hz. The radiometer field stops provided with the instrument were replaced by modified units which accept interference filters to limit the spectral region to which the instrument responded. The transmissivity of the filters is indicated in Fig. 1. Both filters were manufactured by Optical Coating Laboratories, Incorporated.

The radiance fluctuations observed in the ozone band by Adel and Epstein[11] were less than 0.06 mW cm^{-2} sr^{-1}, or three times the NEN of the instrument with $f/2$ optics. This is sufficient signal-to-noise to detect changes if data are collected over a sufficiently long period to isolate true radiance fluctuations from instrumental drift.

To allow better measurements of the solar aureole without sacrificing the NEN, larger aperture optics with the same f/ratio were required. The use of a 61-cm aperture $f/2$ radiometer was provided by ITT Federal Laboratories, San Fernando, California, and the Barnes radiometer head was mounted at the Newtonian focus of this instrument for the aureole studies. To protect the interference filters and bolometers from solar visual and ir energy, and the great heat which would have been generated in the absorbing elements of the filters and bolometer, the entire aperture of the radiometer was masked with two layers of 0.150-mm thick black polyethylene.

Polarization measurements were made with a Perkin-Elmer wire grid polarizer. This component has a clear aperture of 20 mm and consists of strips of vapor-deposited gold with 2880 lines mm^{-1} on a silver bromide substrate. It was not possible to mount the polarizer between the bolometer and chopper because of limited room in the Barnes radiometer design. This militates against absolute polarized radiometry, but the degree of polarization may be measured by placing the grid in the $f/2$ beam as it passes through the aperture in the Cassegrain primary. The entire optics were then rotated to measure polarization.

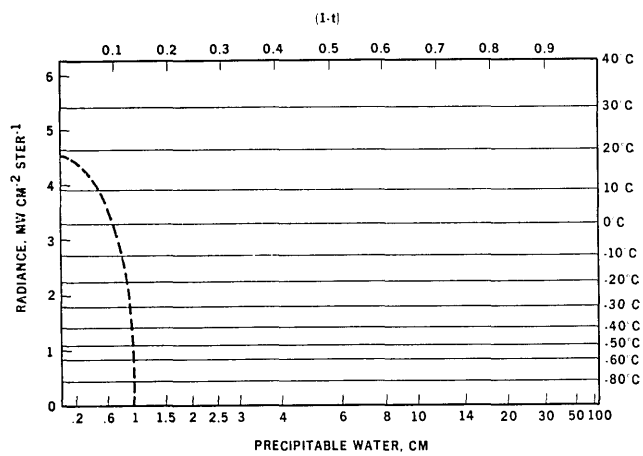

Fig. 2. Simplified radiation chart for the 8.0–13.5-μ window. The construction of the chart is based on that of Bolle, Möller, and Zdunkowski (1963). The dashed line encloses an area representative of zenith sky radiance observed from the ground under typical clear conditions in southern California.

A Model of Window Radiance

In order to compare measurements of sky radiance vs zenith angle for different days, a model of clear sky radiance is required. The need for simplified computational tools has led to the construction of radiation charts for estimating ir absorbing gas and vapor radiance.[12] In constructing his radiation charts, Möller[13] divided the spectrum into twenty-three intervals, each of which was characterized by one synthetic Lorentz line. For the window region from 8.75 μ to 12.25 μ, the synthetic line was described by a half-width $\alpha_0 = 59.5$ cm^{-1} and an absorption constant $k_{\nu_0} = 0.24$ cm^{-1}. A later correction[14] indicates that k_{ν_0} should be nearer to 0.4 cm^{-1} or perhaps even larger. A corrected version of the window radiation chart with $k_{\nu_0} = 0.6$ cm^{-1}, to accommodate the slightly wider spectral region employed in the measurements reported here, is given in Fig. 2 based on the original Möller chart.

In order to use the chart to predict sky radiance, it is necessary to know the vertical distribution of water vapor and temperature. The total amount of precipitable water below a given isotherm is plotted on the appropriate ordinate line, so that for the higher levels at lower temperature, the locus of precipitable water becomes asymptotic to the abscissa value, which represents the total precipitable water above the level of reference. Thus, to predict zenith radiance observed from the ground, the plot will start at the ground level temperature and 0 cm precipitable water. The plot then will curve downward as illustrated by the dashed line in Fig. 2, typical of daytime plots for clear winter days in southern California.

An atmospheric window radiance model must also consider the effect of tropospheric aerosols. Robinson,[5] and Roach and Goody[15] have clearly shown the strong influence haze can have on the magnitude and spatial distribution of window radiance.

In order to compute the absorptance, emittance, and scattering of haze, the properties of individual particles must be understood. Mie scattering properties of spheres for a large range of size parameters, and with index of refraction and absorption constant typical of water for the ir, have been calculated to a high degree of accuracy.[16] Deirmendjian[17] has utilized these calculations and representative aerosol distributions to compute the ir properties of haze and cloud models for wavelengths from 0.45 μ to 16.6 μ. His M haze was chosen to agree with aerosol particle counts made in Los Angeles.

The extinction coefficient is a function of the index of refraction m, a complex quantity for water in the 8–13-μ window, as well as wavelength and particle concentration. Deirmendjian finds for his haze M that the 8–13-μ window extinction is less than 0.1 of the visual extinction. This type of decrease has been measured by Yates and Taylor[18] whose data show that the knowledge of the visual extinction coefficient allows for predicting the infrared characteristics within a factor of approximately two.

The meteorological range MR (Ref. 19) may be related to the visual extinction coefficient by

$$MR = 3.912/k_{\text{ext}}. \quad (1)$$

In this manner, it is possible to extrapolate to the ir extinction coefficients for those radiometric studies where visual range is reported, as does Robinson.[2] He took no measurements when the visibility, interpreted here to mean meteorological range, was less than 1000 yd (914 m). MR of 1000 yd implies a visual extinction coefficient of $k = 4.27$ km^{-1} or an 8–13-μ coefficient of approximately $\frac{1}{10}$ this value. The transmittance for window radiation incoming from the zenith through a haze layer, taken to have an effective height of 1 km, somewhat less than typical,[20] would then be $t = 0.65$. Infrared flux from sources high in or above the atmosphere would thus be attenuated by $(1 - t)$ or 0.35 at the earth's surface due to such a low lying haze.

Emission from this aerosol haze would provide additional flux at the earth's surface. The layer would be approximately isothermal at a value near sheltered air temperatures at the earth's surface. The average 8–13.5-μ albedo of the M haze is $\omega = 0.21$, making the radiant absorptance $1 - 0.21 = 0.79$. In the lower atmosphere, the pressure is high enough so that Kirchhoff's law is valid, and each volume element of the haze absorbs and emits radiation in equal amounts. Then the haze emittance ϵ is related to the transmittance t by:

$$\epsilon = (1 - \omega)(1 - t) = 0.79 \times 0.35 = 0.28. \quad (2)$$

For an air temperature of 290°K, the haze will then have a window radiance of 1.2 mW cm^{-2} sr^{-1}.

It is more difficult to construct an heuristic model of scattering effects for aerosols, since the scattering phase function will not be isotropic as is the emission function. However, since the haze scattering albedo is 0.21 in the window and since forward scattering will predominate due to the strong influence of the larger aerosols in the haze distribution, it can be argued that scattering of earth radiance in the backward direction should be less than 0.21 of the emission effects, leading to only slight scattered sky radiance as compared with this passive thermal radiation, even for the MR of but 1 km.

It is now of importance to determine whether the low lying aerosols can significantly affect window measurements under much less turbid conditions than MR of 1 km. Consider measurements conducted when the MR is 50 km. The visual extinction coefficient is then 7.8×10^{-2} km^{-1} and the 8–13-μ window extinction $\sim 7.8 \times 10^{-3}$ km^{-1}. This latter extinction corresponds to ir transmittance through a 1-km haze layer of better than 0.999. The emittance of the layer for the highly absorbing particles is then 8×10^{-4}, leading to an aerosol window radiance of 3.7×10^{-6} W cm^{-2} sr^{-1}, a value far below the noise equivalent radiance of a bolometer-equipped radiometer. It may thus be concluded that for a visual range of 50 km, the radiation chart, considering emission from water vapor and CO_2, should be adequate to describe window radiance in the absence of other radiation sources.

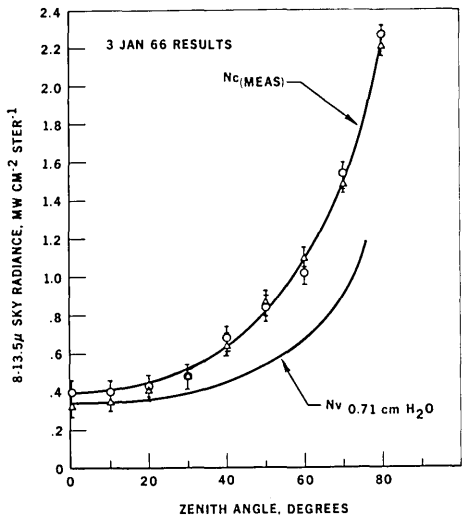

Fig. 3. Sky radiance results, 3 January 1966.

Sources of Excess Sky Radiance

Strong[1] proposed time varying amounts of oxides of nitrogen, CO_2, hydrocarbons, or formaldehyde, but this now seems to be an unlikely cause of the excess. The measurements of Migeotte *et al*[21] have shown only weak absorption lines due to H_2O, CO_2, CH_4, N_2O, and HDO in the window, as well as the more intense O_3 bands. Little variation is found in the absorption due to the weak lines from day to day, completely insufficient to account for the observed anomalies.

Long-term fluctuations in the 9.6-μ ozone band radiance have been measured by Adel and Epstein,[11] where a variance of several degrees Kelvin was determined. This would lead to window irradiance changes from the entire sky of less than 0.2 mW cm^{-2}, or less by an order of magnitude than the fluctuations noted by Robinson.[2]

Robinson[5] attributed excess radiation which increased with zenith angle to radiation from turbid layers high in the atmosphere, and considered that these might be tenuous and uniform high clouds. In order to discuss the radiance caused by thermal emission and scattered earth emission in thin cirrus clouds, it is first required to establish the optical parameters which describe such clouds. Thus the size distribution of the ice particles, the optical thickness of the layer, and the optical constants of ice must be known.

One of the most comprehensive studies of cirrus clouds has been reported by Weickmann.[7] In this investigation, cirrus particles were collected on coated slides from an open aircraft at altitudes to 10,000 m. A typical cirrus particle might be a prism 200 μ in length, 30 μ wide, or equivalent to a 50-μ radius sphere, with an average particle concentration of 5×10^5 m^{-3}. Even for wavelengths of 12 μ within the window, the large size of the cirrus crystals leads to a size parameter $x = 2\pi a/\lambda = 26$.

The optical constants for ice have been calculated by Kislovskii.[22] Throughout the window from 8.0 μ to 13.5 μ, ice has a complex index of refraction. Values of $m = 1.18 - 0.2i$ to $m = 1.56 - 0.5i$ will be encountered. No angular scattering characteristics for particles with a size parameter of twenty-six for the above range of complex indices seem to be available, although for the smaller size parameter $x = 10$ calculations have been performed for several complex indices in the range of interest noted above.[16]

The preceding paragraphs have indicated that although it is possible to construct a physical model of a cirrostratus cloud consisting of nearly monodisperse, 50-μ radius ice spheres based on Weickmann's work,[7] the lack of accurate scattering diagrams does not allow a complete radiative transfer theory of cirrus cloud radiance to be calculated. Such a calculation is an exceedingly complex task, beyond the scope of this experiment study. The task is even more difficult for convective cirrus clouds, where typically bundles of crystals are found of complex shape which are probably not well approximated by an equivalently sized ice sphere. For these reasons only general statements can be made about the ir properties of cirrus. Owing to the large absorption constant, ice crystals are essentially opaque from 8–13-μ, since a $1/e$ attenuation of ir radiation occurs in but several microns of passage through the particle. Thus we will not expect to find ir halos or other refractive effects.

The large size parameter even at ir wavelengths leads to strong forward scattering which, owing to the opacity of the particle, should be well approximated by the diffraction theory. The diffraction pattern may be calculated, and for a size parameter $x = 26$, the first minimum is found at a scattering angle of 8.4°.

Another characteristic of light scattered from large, absorbing particles may be determined by studying the calculations of Plass,[23] who shows that for increasing absorption in particles (at least up to size parameter $x = 8$) scattered light polarized perpendicular to the scattering plan will be of greater intensity than that polarized parallel to the scattering plane. The scattering angle for the maximum positive polarization ap-

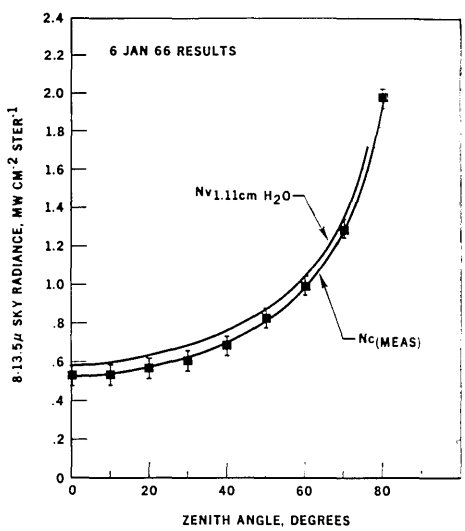

Fig. 4. Sky radiance results, 6 January 1966.

proaches that predicted by the Brewster angle. This same characteristic has been noted by Deirmendjian *et al.*,[16] who state that when the scattering contribution of light transmitted through the particles is suppressed by absorption, "The positive polarization of the externally reflected ray dominates the scattered field."

The question of how thin a cirrus can be detected by the ground-based observer has yet to be convincingly answered. Certainly the unaided observer is unable to distinguish a very uniform, high level haze from one lower in the troposphere, unless halos or parhelia are present.

Although the extinction efficiency of cirrus particles in the visual region will be of the order 2.0, Gumprecht and Sliepcevich[24] properly point out that the predominance of forward scattering makes it difficult or impossible to distinguish the scattered radiation from the directly incident flux. For example, the $a = 50\ \mu$ ice sphere chosen as a typical cirrus particle will have a visual size parameter greater than 500. Mie theory calculations show that for such a large size parameter, one-half of the energy will be within a scattering angle of 1.4° from the source, so that at most an extinction efficiency of $Q = 1.0$ should be used. An $l = 200$ m thick cirrus haze model composed of $n = 5 \times 10^4$ m^{-3} particles of radius $a = 50\ \mu$ will then have an optical depth $\tau = \pi a^2 Q n l = 0.086$ or a transmittance of 92%. The unaided observer would hardly be able to recognize this slight decrease in solar illuminance, and, unless irregular structure were present in the cloud, would be unaware of its presence. He might notice a slight milkiness to the zenith sky, if the visual range at his location were sufficiently great to make the effect discernible. The common occurrence of thin cirrus or cirrus haze has been documented by Stone,[25] who states that extensive sheets of ice clouds can occur in tropical, temperate, and polar regions much more often than the ground-based observer reports. A cloud 200 m thick but with ten times the particle density will directly transmit but 42% in the visual region, and should be detectable.

Sky Radiance Measurements

In this section, 8–13.5-μ sky radiance measurements plotted vs zenith angle are compared with the radiation chart predicted radiance. Clear sky and cirrus haze conditions are discussed first; cirrus clouds are discussed thereafter. A more complete atlas of measurements may be found in the dissertation upon which this paper is based.[26]

The lowest zenith radiance measured during the investigation occurred on 3 January 1966. In Fig. 3, a smooth curve has been drawn through the 0520-h (⊙) and 1210-h (△) data, from which ozone band radiance has been subtracted using the 9.6-μ spike filter radiance values. This curve may be compared with the lower solid curve which shows radiance predicted from the radiation chart, Fig. 2. The radiation chart radiance is based on 0500 h Los Angeles International Airport (LAX) radiosonde data, but if the 1200-h surface temperature is used instead for the lowest levels of tropospheric water vapor, predicted zenith radiance increases

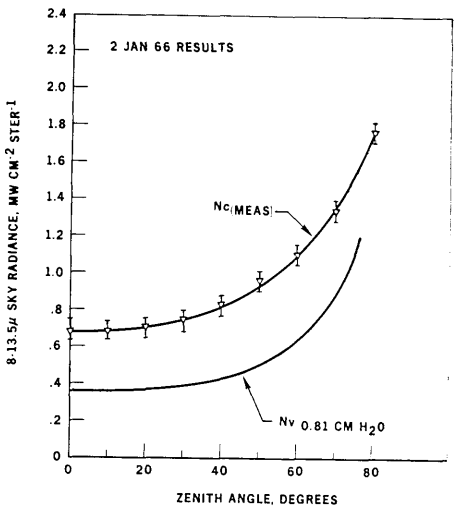

Fig. 5. Sky radiance results, 2 January 1966.

by only 0.02 mW cm^{-2} sr^{-1}, or about the width of the line on the graph. It is not surprising, therefore, that the sky radiance values did not change significantly from before sunrise to noon. There was a large aureole on 3 January, which may have been visual evidence of a cirrus haze, since the lower 2 km of the atmosphere was very clear, with $MR > 50$ km.

On 6 January 1966, when the aureole was much smaller, and $MR > 50$ km, the measured radiance was slightly lower than that predicted from the radiation chart, as shown in Fig. 4. Apparently there was a negligible radiance contribution from cirrus on this day, and the 10–20-knot (5–10-m/sec) wind from the northwest may have brought drier air to San Fernando than the 1.11-cm H_2O at LAX. The Santa Monica Mountains frequently provide a wind screen for the airport area, with the marine layer providing more low level moisture there than in the inland valleys under such wind conditions. The close fit in curvature of the measurements and radiation chart curves does substantiate the accuracy of the Möller chart. Short-term zenith radiance fluctuations on 6 January averaged 0.02 mW cm^{-2} sr^{-1}, compared with 0.07 for 3 January, pointing out the probable cirrus haze contribution to sky radiance variability.

The results of the 2 January 1966 data and model comparison are given in Fig. 5. Cirrus could be seen in the aureole occasionally, $MR > 50$ km, and there was 0.81 cm of precipitable water. From these results, we hypothesize that if cirrus cloud forms are detected in the aureole, or if clear sky parhelia are seen, sky radiance may exceed considerably the radiance predicted from tropospheric water vapor. A cirrus haze without these clues is thus difficult for the unaided ground-based observer to detect.

In Fig. 6, the cirrus haze to thin cirrus overcast conditions of 4 January 1966 are shown. Cirrus were not unambiguously detected until twilight when pink cloud streaks clearly showed. The low haze on this date, which limited the MR to 15 km at 1245, and 25 km at 1525, added to the difficulty in visual detection as well

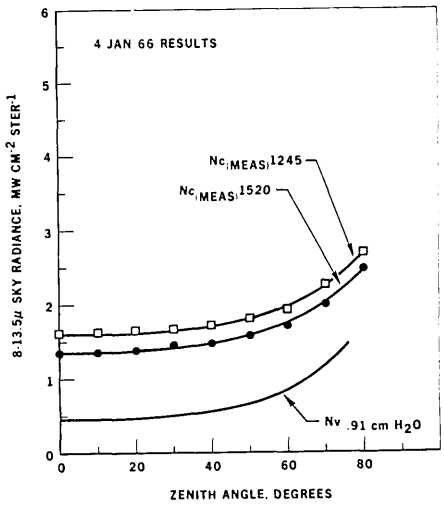

Fig. 6. Sky radiance results, 4 January 1966.

as contributing an excess ir radiance. This serves to explain the experiences of Robinson,[2] where apparently clear days (near typically hazy London) sometimes exhibited excess total sky irradiance of 3 mW cm^{-2}.

On days with clearly observable cirrus clouds, it might be expected that radiance should significantly exceed that predicted from the radiation chart. Measurements at 1440 h on 7 January 1966 under broken cirrus fibratus and cirrostratus do exceed the model, as illustrated in Fig. 7. Later, at 1630, the clouds had thickened, all but eliminating any blue sky, and radiance correspondingly increased, except near the horizon. These clouds were undoubtedly thicker than 200 m, and it is not unexpected that the chart radiance prediction is far too low.

The cirrus radiance measurements of 20 September 1966 sampled a great range of cirrus sky conditions. The two morning measurements under broken cirrus fibratus, the upper curves in Fig. 8, greatly exceed the chart radiance. However, the 1240 measurement, made against widely scattered, tenuous cirrus uncinus, lies closer to the chart prediction, except near the horizon where the clouds were thicker. On another occasion, when an isolated cirrus uncinus cloud drifted slowly through the zenith field of view on 20 September 1966 it produced a transient excess radiance of 0.1 mW cm^{-2} sr^{-1}.

Measurements of the Solar Aureole

There is little limb darkening to be expected on the sun at 10 μ. Less than 5% darkening would be expected 95% of the distance from the center of the sun to the limb, as measured across the apparent disk.[9] However, the radiometer image spread function will influence the radiance profile of the sun, and instead of a sharp edge, a more rounded recording of radiance against the sky would be expected. A typical profile measured at a zenith angle of 55° is shown in Fig. 9(a). The less than rectangular aspect of radiometer deflection is to be expected because of instrumental effects but would also be experienced if forward scattering were occurring in the earth's atmosphere.

It may be shown that if solar transit deflections for different zenith angles are normalized to the same deflection, any difference in shape of the deflection recorded vs time reveal scattering which is independent of the instrument and thus provide a true measure of the infrared solar aureole. Shown in Fig. 9(b) is the transit for a zenith angle of 85°, both scans having been taken on 6 January 1966. It will be noted that for the larger zenith angle, radiance is greater outside of the solar limb, and the limb has a more rounded appearance because of the energy scattered into the aureole.

Subtracting curve (A) from curve (B) gives the excess radiance experienced at the larger zenith angle. This enables a plot to be made of the relative shape of the scattering diagram. In Fig. 10, this has been done for the 6 January 1966 data; the general shape of the experimental curve is similar to the zero-order diffrac-

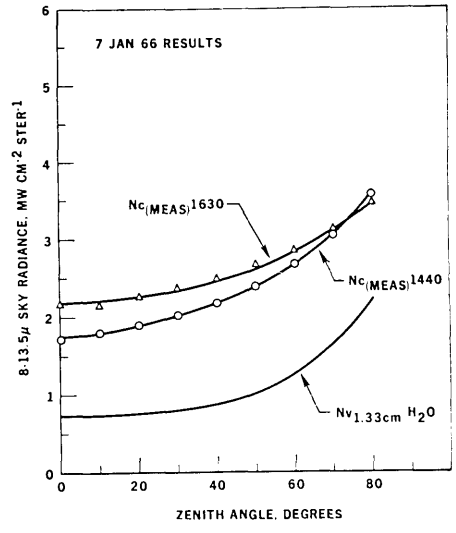

Fig. 7. Sky radiance results, 7 January 1966.

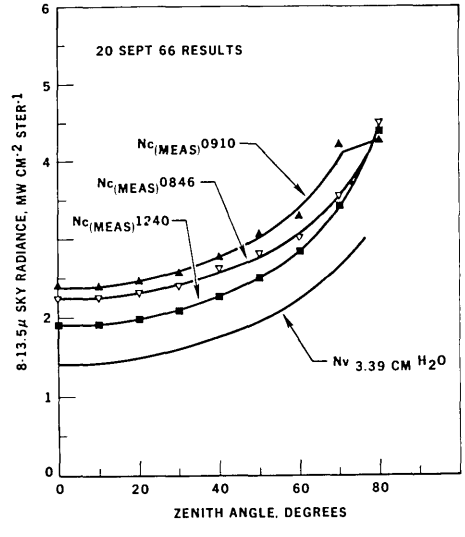

Fig. 8. Sky radiance results, 20 September 1966.

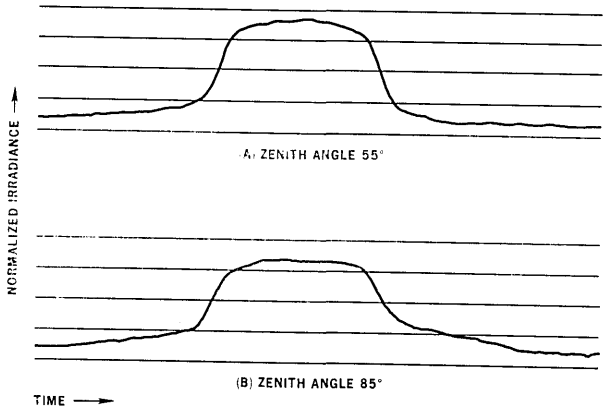

Fig. 9. Recordings of solar transits on 6 January 1966 with the 61-cm radiometer. Deflections have been normalized to the same value at the center of the sun.

tion diagram for a 50-μ radius sphere, but is restricted to smaller scattering angles.

Polarization of Sky Radiance

The experimental procedure for measuring polarization was to point the radiometer at various azimuth and zenith angles, and slowly rotate the polarizer through 360°. Orientation of the polarizer was noted on the paper tape from the data recorder as the measurements were being made.

On 1 February 1967, no polarization was detectable in the 8–13.5-μ channel under a thick cirrostratus nebulosus overcast (faint shadows, weak 22° halo). Surprisingly, the second channel filtered with a germanium window (the 9.6-μ filter was removed) to provide response at wavelengths longer than 2 μ showed a negative degree of polarization of $P = -0.12$ at zenith angle $\zeta = 60°$N.

The failure to detect polarization from the thick cirrus might be expected because of the importance of multiple scattering in these clouds. Zenith angle changes in radiance were not detectable from $0° < \zeta < 60°$, because of the uniformly high emittance of this layer.

The sky on 2 February was cloudless and clear, with meteorological range greater than 50 km and less than 1 cm of precipitable water in the vertical column. At $\zeta = 60°$N, a definite polarization was noted in the 8–13.5-μ window of value $P = 0.02$, while in the germanium filtered channel, $P = -0.09$. These measurements were obtained at 0748 h, and later on the same day at 1415 h, with cirrus forming in the west, the polarization values were essentially unchanged.

Polarization at the zenith was undetectable in the morning and afternoon of 2 February in the window, but the germanium filtered channel showed a zenith polarization $P = -0.03$ at 0748 h, and $P = -0.01$ at 1415. Measurements at azimuths ranging around the compass showed the 8–13.5-μ polarization to be essentially independent of this variable on this very clear day. Polarization increased from zero at the zenith to a maximum at $60° < \zeta < 70°$, indicating that the polarized radiation was due to scattering of emission from the earth.

The germanium filtered channel was not azimuth independent, and was influenced by the position of the sun. Polarization values were approximately symmetric about the sun's vertical, indicating that this channel was probably measuring polarization due to near ir scattered sunlight.

On 3 February, a Santa Ana wind was present, which gave rise to cirrus wave clouds over the San Gabriel Mountains. A series of measurements of sky polarization was made on the visible cirrus and in the clear sky 10° to the east. The visual range exceeded 100 km. The 8–13-μ polarization on the cirrus clouds was found to be $P = 0.05$; while in the clear sky adjacent to the clouds, the polarization was $P = 0.04$. The clear sky to the south over the ocean measured $P = 0.03$ with a probable error in all measurements given of ± 0.005. However, in the germanium filtered channel the cloud polarization was -0.05, while clear sky at the same zenith angle was -0.06.

The larger polarization values obtained on 3 February made it possible to determine the plane of 8–13.5-μ polarization symmetry. For the cirrus clouds, this plane was vertical to within ±15°. Elsewhere in the apparently clear sky, symmetry occurred about a vertical plane to within ±20°.

The prediction made for positive polarization of earth radiance scattered by cirrus clouds is supported by the reduced data. The maximum value measured was 0.04. The slight but detectable decrease in polarization over the ocean as opposed to over land may have been due to the negatively polarized radiance of water at large zenith angles.[27]

Conclusions

Prior to this investigation, the explanation of excess and fluctuating window radiance on clear days pointed strongly to effects of turbid layers or thin clouds. Gaseous or vapor emission has now been eliminated

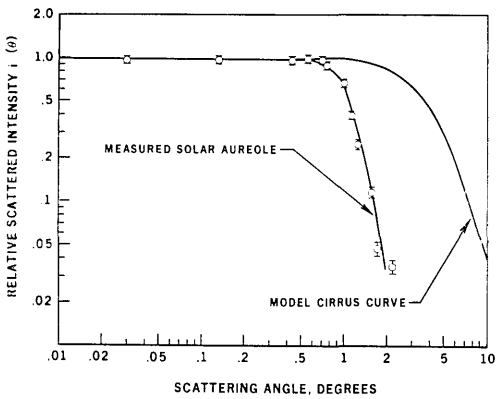

Fig. 10. Relative scattered intensity $i(\theta)$ vs scattering angle θ. The measured, normalized aureole radiance at 8.0–13.5-μ is indicated by the flagged points and compared vs scattering angle with the zero-order diffraction diagram for 50-μ radius spheres.

by spectrographic studies and the ozone band data gathered early in this investigation.

A radiation chart has been used to predict the zenith angle dependence of radiance due to tropospheric water vapor. In all but one case the radiation chart underestimated sky radiance, and for all cases when cirrus clouds were clearly present, the excess was greater than 1 mW cm^{-2} sr^{-1} within the 8–13.5-μ window. The excess in general increased with zenith angle. On days when only a possibility of cirrus being present was noted, for example, by a large and filmy aureole, faint parhelia, or cirrus near the horizon, the excess zenith radiance was from 0.1 mW cm^2 sr^{-1} to 0.5 mW cm^{-2} sr^{-1}, even with a highly transparent lower atmosphere with meteorological range greater than 50 km.

Forward scattering from the large cirrus particles can lead to an 8–13.5-μ aureole of measurable radiance close to the sun. It is believed this is the first detection of the aureole at this long wavelength. The aureole is not detectable on all days; it is easily detectable when visible cirrus are present, but, owing to scattering effects within the instrument, it is necessary to compare radiance readings made at different zenith angles to prove its presence unambiguously for any one set of measurements.

Polarization of sky radiance in the 8–13.5-μ window has also been detected for the first time. It is hypothesized that this positive polarization might be characteristic of scattering from ice particles in the window due to the importance of reflection from the surface of the particles over internally transmitted rays. Thin visible cirrus lead to greater polarization than apparently clear sky near such cirrus, and on days when no clouds are present, somewhat less polarization is found. In addition, less polarization is observed in the sky over the ocean, where the negatively polarized emission from this smooth specular surface leads one to predict this effect.

Sky radiance fluctuations observed to correlate with the passage of visual cirrus through the radiometer's field of view are of the correct time distribution to explain such fluctuations observed by previous investigators.[3]

A more complete proof that thin cirrus are causing the observed radiance distributions would be obtained by directly measuring cirrus thickness and extent. Such measurements might be made using a ground-based pulsed laser to probe the clouds. Better data on cirrus particle shapes, sizes, and spatial distributions would also be helpful, since this would allow an exact Mie theory of the scattering properties of such particles to be numerically evaluated. The phase function so obtained for particle distributions in real cirrus clouds would then allow solution of the complete equations of radiative transfer to provide a quantitative model against which to compare radiance measurements such as those reported here.

Basically, the conclusions drawn above are due to one simple fact: cirrus ice particles are quite large compared with cloud water droplets, and therefore the size parameter is still large for 12-μ ir wavelengths and the extinction efficiency remains high, of the order two. The large size parameter, together with the absorbing properties of ice in the 8–13-μ window causes cirrus to have an easily measured influence on sky radiance and necessarily, therefore, an influence on the heat budget of the earth.

It is a pleasure to acknowledge the counseling and guidance of Z. Sekera at UCLA throughout the course of this investigation. Many discussions with S. V. Venkateswaran were also very helpful. One of the referees has kindly pointed out that a paper by W. M. Irvine and J. B. Pollack, to be published in *Icarus*, finds the absorption constant for ice in the 8–13-μ region to be less than that given by Kislovskii. These lower values are still large enough to rule out pronounced ir halos or other refractive effects.

References

1. J. Strong, J. Franklin Inst. **232,** 1 (1941).
2. G. D. Robinson, Quart. J. Roy. Meteorol. Soc. **73,** 127(1947).
3. J. Westphal, Mem. Soc. Roy. Sci. Liege **9** (Ser. 5), 357 (1964).
4. H. J. Bolle, Final Rept. AF61(052)–488, AFCRL–64–567 II (AD 623 406) University of Munich (1965).
5. G. D. Robinson, Quart. J. Roy. Meteorol. Soc. **76,** 37 (1950).
6. C. B. Farmer and P. J. Key, Appl. Opt. **4,** 1051 (1965).
7. H. Weickmann, Ber. Deut. Wetter. U. S. Zone **6,** 61 (1949).
8. S. Chandrasekhar, *Radiative Transfer* (Dover Publications, Inc., New York, 1960), p. 248.
9. M. Minnaert, in *The Sun*, G. Kuiper, Ed. (The University of Chicago Press, Chicago, 1953) pp. 102, 130.
10. H. C. van de Hulst, in *The Sun*, G. Kuiper, Ed. (The University of Chicago Press, Chicago, 1953), p. 246.
11. A. Adel and E. S. Epstein, J. Meteorol. **16,** 548 (1959).
12. R. M. Goody, *Atmospheric Radiation* (Oxford University Press, London 1964), p. 249.
13. F. Möller, *Nomogramme für den Reichswetterdienst, Reichsamt für Wetterdienst* (Springer-Verlag, Berlin, 1943), pp. 38–43.
14. H. J. Bolle, F. Möller, and W. Zdunkowski, Tech. Rept. No. 2, AF 61 (052)–488, AFCRL–63–680 (AD 416 497) University of Munich (1963).
15. W. T. Roach and R. M. Goody, Quart. J. Roy. Meteorol. Soc. **84,** 319 (1958).
16. D. Deirmendjian, R. Clasen, and W. Viezee, J. Opt. Soc. Am. **51,** 620 (1961).
17. D. Deirmendjian, Appl. Opt. **3,** 187 (1964).
18. H. W. Yates and J. H. Taylor, NRL Rept. 5433 (1960).
19. W. E. K. Middleton, *Vision Through the Atmosphere* (The University of Toronto Press, Toronto, 1952), p. 104.
20. K. Bullrich, in *Advances in Geophysics*, H. E. Landsberg and J. van Miegham Eds. (Academic Press, Inc., New York, 1964), Vol.10.
21. M. Migeotte, L. Neven and J. Swensson, The Solar Spectrum from 2.8 to 23.7 Microns, University of Liege Final Rept., AF 61 (514)–432 (AD 210 043, 210 044) (1957).
22. L. D. Kislovskii, Opt. Spectrosc. **7,** 201 (1959).
23. G. N. Plass, Appl. Opt. **5,** 279 (1966).
24. R. O. Gumprecht and C. M. Sliepcevich, J. Phys. Chem. **57,** 90 (1953).
25. R. G. Stone, USAF Air Weather Service TR 105–130 (1957).
26. F. F. Hall, Jr., Ph.D. Dissertation, UCLA (1967), also Douglas A/C Report DAC–61306.
27. F. F. Hall, Jr., Appl. Opt. **3,** 781 (1964).